Article

Not by Serendipity: Rationally Designed Reversible Temperature-Responsive Circularly Polarized Luminescence Inversion by Coupling Two Scenarios of Harata–Kodaka's Rule

Xuejiao Wang, Wanwan Zhi, Cheng Ma, Zhiyang Zhu, Weilin Qi, Jianbin Huang, and Yun Yan*

Read Online

ACCESS | Metrics & More | Article Recommendations | SI Supporting Information

ABSTRACT: Intelligent control over the handedness of circularly polarized luminescence (CPL) is of special significance in smart optoelectronics, information storage, and data encryption; however, it still remains a great challenge to rationally design a CPL material that displays reversible handedness inversion without changing the system composition. Herein, we show this comes true by coupling the two scenarios of Harata−Kodaka's rule on the same supramolecular platform of crystalline microtubes self-assembled from surfactant−cyclodextrin host−guest complexes. Upon coassembling a linear dye with its electronic transition dipole moment outside of the cavity of β-CyD, the chirality transfer from the induced chirality of SDS in the SDS@2β-CyD microtubes to the dye generates left-handed CPL at room temperature. Upon elevating temperature, the dye forms inclusion complex with β-CyD, so that right-handed CPL is induced because the polar group of the dye is outside of the cavity of β-CyD. This process is completely reversible. We envision that host−guest chemistry would be very promising in creating smart CPL inversion materials for a vast number of applications.

KEYWORDS: cyclodextrins, circularly polarized luminescence, Harata−Kodaka's rule, self-assembly, host−guest
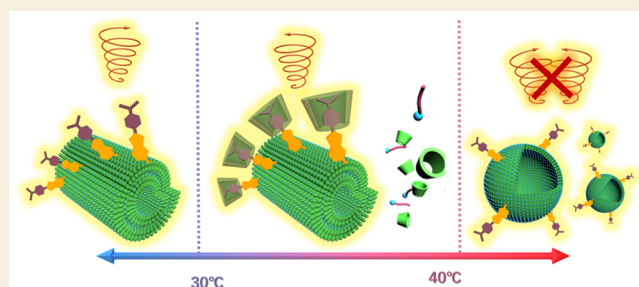
INTRODUCTION

The origin of chirality at different scales is one of the top puzzles of nature. Of special puzzle is the stimuli responsive structural chirality inversion. For instance, the newborn tendrils of many plants are nonspiral, but they develop spiral structures when they encounter a stick which they can twine around. To release the tension generated by spiral, inversion of the spiral handedness occurs. So far, scientists are able to create various chiral spiral structures via molecular self-assembly[1,2] or via macroscopic fabrication procedures,[3−5] but it still remains a great challenge to endow various chiral structures at different scales with stimuli responsive handedness inversion.

It is well-known that cyclodextrins (CyDs) are doughnut ring-like oligosaccharides capable of forming host−guest complexes.[6,7] Because the cavities of CyD are chiral, the chirality of CyDs can be transferred to the guest through dipole−dipole interaction between the transition moment of a guest molecule and the bonds composing the chiral host β-CyD.[8−14] In 1970s and 1990s, Harata[15,16] and Kodaka[17,18] et al. figured out that the induced chirality of the guest is closely related with the relative location of the chromophore and orientation of its electronic dipole transition moment to the cavity of CyD. For a guest with its electronic dipole transition moment orientation parallel to the axis of the cavity of CyDs, the induced CD signal (circular dichroism spectrum) would be positive if the chromophore is inside the cavity; otherwise, it is negative (Figure S1).[19] In the past half-century, this principle is mainly utilized to understand the induced supramolecular chirality,[20−23] but it has not been sufficiently employed in creating smart chirality inversion materials.

Intelligent circularly polarized luminescence (CPL) has promising applications in a number of important fields, such as photoelectronics,[24−27] three-dimensional displays,[28,29] and data recording.[30,31] Intelligent control over the CPL handedness is of special significance in smart optoelectronics, information storage, and data encryption.[32,33] So far, switching of the CPL handedness is achieved by controlling the system component, such as enantiomers,[34,35] solvent,[36−38] coordinating metal ions,[39] solution pH,[40] redox reaction,[41−43] or other alien chemicals.[44−47] Despite the significant progress, inversion of CPL handedness requires changing the composition of the systems, which prohibits their application as smart CPL materials. Although some wonderful external stimuli respon-

sive CPL handedness inversion systems have been reported,[48−52] most of them are serendipitous discoveries. It still remains a great challenge to rationally design smart CPL inversion materials without changing the component of the CPL system.[53]

Herein, we report that upon coupling the two scenarios described in Harata−Kodaka's rule, rational design of temperature-responsive CPL inversion becomes possible. The achiral fluorescent dye ThT, which displays chiral environment dependent CPL,[54] was coassembled on the surface of the crystalline self-assembly of SDS@2β-CyD microtubes (Scheme 1a, b). Chirality transfer from SDS to ThT leads to left-handed

Scheme 1. Illustration of (a) the Formation of the Crystalline Self-Assembly of SDS@2β-CyD Microtube,[a] (b) the Coassembly of Fluorescent Dye ThT with the Microtube,[b] and (c) Temperature-Triggered CPL Inversion in the System of ThT- SDS@2β-CyD Microtubes[c]
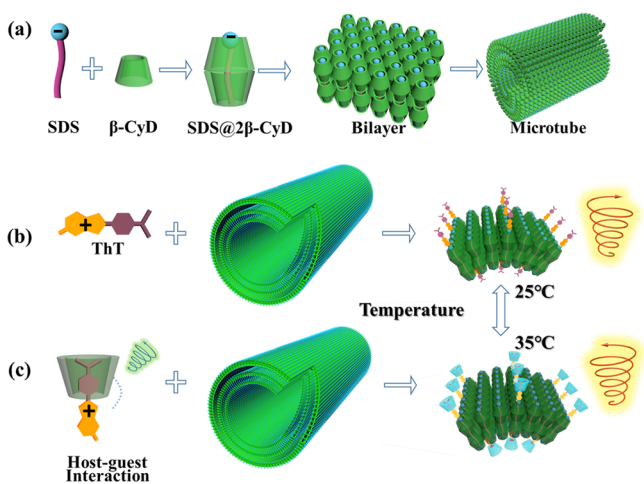
[a]Two β-CyD hosts lock one SDS molecule and form the host−guest building block of SDS@2β-CyD, which in turn assembles into bilayers, thereby forming chiral microtubes. [b]ThT is highly oriented to the surface of the microtubule via electrostatic interaction, allowing the appearance of left-handed CPL. [c]Temperature triggered self-assembly transition and the host−guest complexation between β-CyD and the dye, inducing CPL inversion.

CPL because the sulfate group, which is the chromophore of SDS, is inside the cavity of β-CyD. However, increasing temperature from 25 to 35 °C triggers the host−guest complexation between the hydrophobic part of ThT and β-CyD, leaving the positive charge of ThT outside (Scheme 1b, c). Consequently, the induced chirality inversion of the dye occurs on the surface of the microtubes, which leads to CPL inversion without changing the system composition. Further increase of temperature to above 40 °C results in significant disassembly of the SDS@2β-CyD microtubes, and CPL vanishes. This temperature-responsive host−guest chemistry and the self-assembly transition is completely reversible. As such, intelligent dynamic CPL materials displaying multimode temperature responsiveness is thus generated. We envision that the current work may pave the way for the design of intelligent chiral materials.

EXPERIMENTAL SECTION

Chemicals

Sodium dodecyl sulfate (SDS, 99%) was purchased from Acros Organics Co. and used as received. The purity of SDS was tested by the absence of minimum in its surface tension curve. β-Cyclodextrin (β-CyD), Rhodamine B (RhB), and Acridine orange (AO) were purchased from Sinopharm Chemical Reagent Co., Ltd. with a water content of 14%. Thioflavin T (ThT) was purchased from TCI. Distilled water was purified through Milli-Q Advantage A10 Ultrapure Water System.

Preparation of Microtubes and Coassembly of Dye with the Microtubes. Desired amounts of SDS, β-CyD, and water were weighed into a vessel to give a mixture with a total concentration of SDS and β-CyD of 10 wt % and a molar ratio between SDS and β-CyD of 1:2. The mixture was heated to ∼60 °C to obtain a transparent, isotropic solution, which was then cooled to room temperature to allow for the formation of microtubes. For coassembly experiments, desired amount of aqueous solution of dye (ThT, RhB, AO) were added into the vessel before heating.

Circular Dichroism (CD) Measurements. CD spectra were obtained on a JASCO J-810 spectrometer and used to investigate the chirality of the sample suspension. The light path of the quartz cell is 0.05, 0.1, or 1 mm, depending on different measuring purposes.

Circularly Polarized Luminescence (CPL) and Fluorescence Measurements. CPL spectra were obtained with a JASCO CPL-200 spectrometer. The light path of the quartz cell is 2 mm. The excitation wavelength for ThT and RhB systems are both 400 nm. Fluorescence spectra were recorded by a FLS 920 spectrometer (Edinburgh Instruments Ltd., UK).

Nuclear Magnetic Resonance (NMR) Studies. ^{1}H NMR and ROESY spectra experiments were performed on a Bruker ARX 500 MHz spectrometer at room temperature (25 ± 2 °C) using 5 mm standard NMR tubes.

Transmission Electron Microscopy (TEM) and Freeze-Fractured TEM (FF-TEM) Measurements. A drop of sample (about 30 μL) was loaded on a copper grid, stained with uranyl acetate. TEM images were captured with a JEM-100CX electron microscope. For FF-TEM, samples were frozen by liquid propane; fracturing and replication were carried out in a freeze-fracture apparatus (BalzersBAF400, Germany) at −140 °C. Pt/C was deposited at an angle of 45° to shadow the replicas, and C was deposited at an angle of 90° to consolidate the replicas. The resulting replicas were examined in a JEM-100CX electron microscope.

Confocal Laser Scanning Microscopy (CLSM) Measurements. A drop (about 30 μL) of the sample was sealed between two slides, ready for CLSM observation. A TCS-sp inverted confocal laser scanning microscope (Leica, Germany) was used to conduct experiments in florescence and differential interference contrast (DIC) modes.

Small-Angle X-ray Scattering Instrument (SAXS) Measurements. SAXS measurements were performed by SAXSess (Anton-Paar, Austria, Cu Kα, λ = 0.154 nm), in which samples were sealed in quartz capillary tubes.

Dynamic Light Scattering (DLS) Measurements. A commercialized spectrometer (Brookhaven Instruments Corporation, Holtsville, NY) equipped with a 100 mW solid-state laser (GXC-III, CNI, Changchun, China) operating at 532 nm was used to conduct DLS experiments. Photon correlation measurements in self-beating mode were carried out at multiple scattering angles using a BITurboCo digital correlator. The temperature was held at 60 °C.

ESI-MS Measurements. Electrospray ionization mass spectrometry (ESI-MS) was carried out on an APEX IV FT-MS (Bruker, USA). The operating conditions of the ESI source: positive ion mode; spray voltage 3300 V; capillary voltage 3800 V, capillary temperature 230 °C; skimmer1 33.0 V, skimmer2 28.0 V; sheath gas nitrogen pressure 0.3 bar. The 1 mM alkane/b-CD vesicle samples were diluted 10 times by methanol and introduced via direct infusion at a flow rate of 3.00 mL min^{-1}.
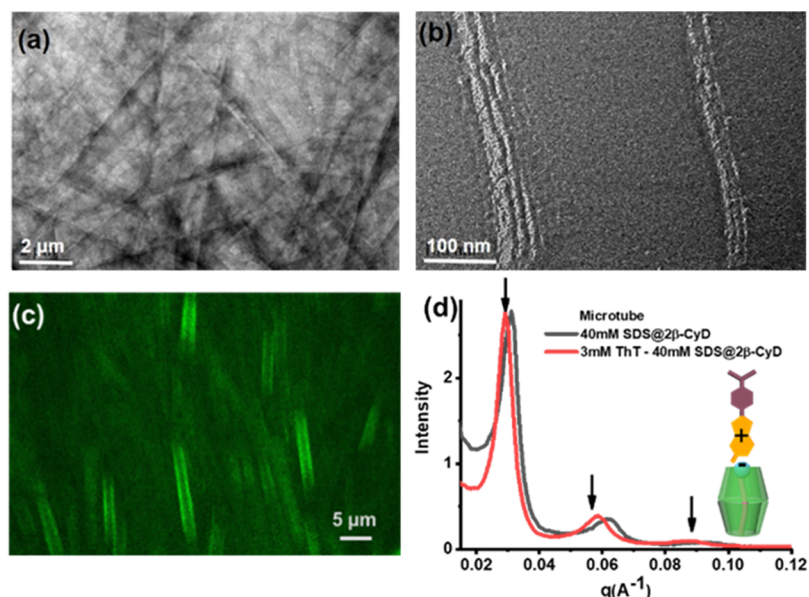
Figure 1. (a) TEM, (b) FF-TEM images, (c) CLSM image, and (d) SAXS profile (red curve) of the microtubes composed of 3 mM ThT and 40 mM SDS@2β-CyD at 25 °C. The black curve in (d) is the SAXS profile of the pristine microtube system of 40 mM SDS@2β-CyD. The inset shows the binding mode of the ThT molecule with the SDS@2β-CyD. The fluorescence in (c) is from ThT under fluorescent mode.
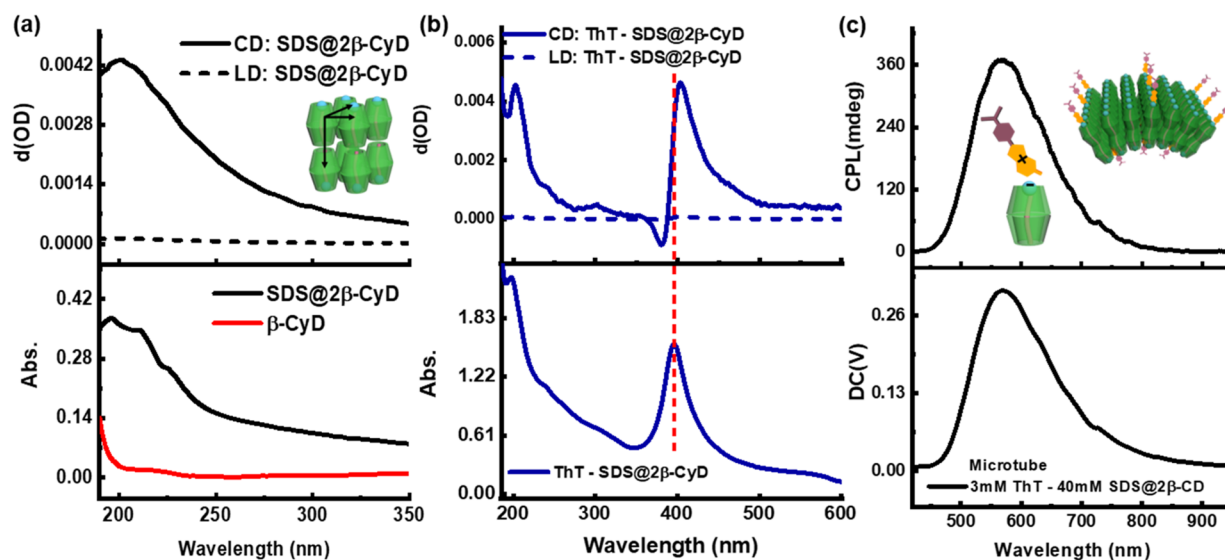

Figure 2. (a) CD/LD (upper) and UV−vis spectra (lower) of 40 mM SDS@2β-CyD microtubes; the inset in the upper panel illustrates the lattice of SDS@2β-CyD in the microtubes; (b) CD/LD (upper) and UV−vis spectra (lower) of the microtubes composed of 3 mM ThT and 40 mM SDS@2β-CyD; (c) CPL spectrum (upper) and direct current mode measurement for the luminescent microtubes. The insets in (c) are the binding mode of ThT on the surface of the microtubes.

■ ¹RESULTS AND DISCUSSION

The crystalline self-assembly of SDS@2β-CyD microtubes, where SDS denotes the surfactant sodium dodecyl sulfate and β-CyD represents β-cyclodextrin (Scheme 1a), were created using methods established in our group.[55] Upon dissolving solid β-CyD into the hot aqueous solution SDS at 60 °C at the stoichiometry of 1:2, inclusion complex SDS@2β-CyD can be formed.[56] On cooling, this supramolecular building block can further self-assemble into vesicles, microtubes, and lamellae driven by hydrogen bonding between β-CyDs.[57] Here, multiwalled microtubes were obtained by cooling the hot aqueous mixture of 40 mM SDS/80 mM β-CyD from 60 to 25 °C. The diameter of the microtubes is about 1−2 μm, but the length is up to 50−100 μm (Figure S2). Addition of 3 mM

cationic fluorescent dye ThT does not influence the size and morphology of the tubes noticeably (Figure 1a, b),[58] but strong fluorescence was observed on the tube walls (Figure 1c). *In situ* SXAS measurements reveal that the scattering peaks in the ThT-SDS@2β-CyD system occur at smaller q values (Figure 1d). The calculated interwall distance d is 20.2 nm in the SDS@2β-CyD system, whereas it increases to 21.8 nm upon addition of ThT. This distance $d = \delta + d_w$, with δ and d_w being the thickness of the bilayer and the water layer between two neighbored tube walls, respectively.[59,60] Because binding of oppositely charged ThT on the tube wall would slightly reduce the thickness of the water layer d_w due to the decreased repulsive forces,[59,60] the increased distance of 21.8 − 20.2 = 1.6 nm should originate from the increased bilayer

thickness δ. Further modulation indicates that this distance of 1.6 nm is close to the length of the ThT molecule (Figure S3). This means that ThT molecules stand on the surface of SDS@2β-CyD using its positively charged head to bind with the negatively charged sulfate group of SDS (inset in Figure 1d). Because the chain length of SDS is 1.45 nm, which is shorter than the two folds of the height of β-CyD (∼0.8 nm), the sulfate group of SDS is inside the cavity of β-CyD. According to Harata−Kodaka's rule, a positive induced CD signal for SDS would be expected. This is experimentally verified by the CD and UV measurements in Figure 2.

Because β-CyD has no absorption in the UV−vis range (Figure 2a, lower panel), the positive signal centered at 200 nm in the CD spectra (Figure 2a, upper panel) corresponds to the absorption of the sulfate group of SDS (Figure 2a, lower panel).[58] Figure 2b shows that upon addition of the positively charged dye ThT to the SDS@2β-CyD microtubes, an extra intensive positive CD signal corresponding to the absorbance of ThT occurs at 405 nm (Figure 2b, upper panel). Because the contribution of possible linear dichroism (LD) on the CD signals can be excluded (Figure S2), this result unambiguously verifies that the induced CD of SDS has successfully transferred to ThT via ionic interaction, in good agreement with literature reports by Duan and Jiang et al.[58] Here, we use this as Scenario I of the Harata−Kodaka's rule in this study. Figure 2c (upper panel) shows that in accordance with the positive induced CD signal of ThT, a positive CPL peaked at 570 nm is observed. This is up to our expectation, because the sign of the lowest energy transition of electronic CD band is the same as the sign for CPL.[61] The emission dissymmetry factor g_{em}, defined as $2(I_L - I_R)/(I_L + I_R)$, with I_L and I_R denoting the emission intensities of left-handed CPL (l-CPL) and right-handed CPL (r-CPL) component, respectively,[62,63] is 0.11, indicating the generation of l-CPL (inset in Figure 2c), which agrees well with Duan and Jiang's study.[58]

Next, we build Scenario II of Harata−Kodaka's rule by direct threading ThT into the cavity of β-CyD. ThT and β-CyD are able to form the host−guest complex of ThT@β-CyD at the molar ratio of 1:1 (binding constant = 78 M^{-1}).[64] 2D NMR measurements suggest that the hydrophobic portion of ThT is threaded into the cavity of β-CyD, leaving the positive charge of ThT outside (Figure 3a). According to Harata−Kodaka's rule,[65] a negative CD signal should be expected. Indeed, the CD measurement in the small window in Figure 3b reveals a weak negative peak at 410 nm. Accordingly, a weak r-CPL is observed at 500 nm (Figure 3b), which is in clear contrast with the strong l-CPL occurring at 570 nm in Figure 2c. However, upon introducing this complex into the system of the SDS@2β-CyD microtubes, the r-CPL redshifts to 570 nm and is amplified 20-fold (Figure 3b) owing to the ionic binding of the host−guest complex to the tubes (inset in Figure 3b).

The reversed induced CD signal of ThT in Scenario I and Scenario II of Harata−Kodaka's rule allows generation of intelligent CPL with temperature responsive handedness inversion. Because the solubility of β-CyD increases sharply with temperature, the crystalline self-assembly tends to disassemble at elevated temperature.[66−68] As a consequence, both the proportion of free β-CyD and SDS in equilibrium with the self-assembled structures increase with increasing temperature. This allows in situ formation of the ThT@β-CyD (1:1) and ThT/SDS complex because ThT has comparable binding ability with β-CyD and SDS (Figures S4−S7).
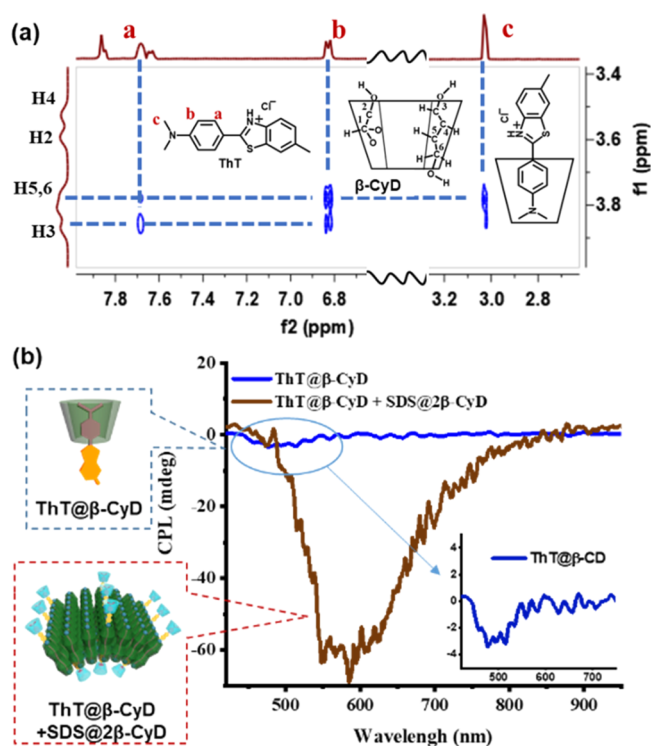

Figure 3. (a) 2D NMR (Roesy, D$_2$O, 298 K) result of ThT@β-CyD (2:2 mM) complex; (b) CPL spectra of the microtubes composed of ThT@β-CyD (2:2 mM) and 40 mM SDS@2β-CyD. The insets are the enlarged CPL for the ThT@β-CyD, the scenario II described by Harata−Kodaka's rule for the host−guest complex of ThT@β-CyD and its binding mode on the tube wall.

Figure 4a shows the progressive variation of the CD signal in the temperature region of 25−40 °C. Considerable CD signal splitting occurs with increasing temperature. The positive signal peaked at 405 nm kept decreasing, whereas a negative one rose up at 395 nm. It was noticed that at 25 °C, the intensity ratio between the negative and positive peak was only 1:12, whereas it increased to 1:1.5 at 40 °C. Strikingly, the splitting between the positive and the negative CD signal does not coincide with the absorption of ThT (the dashed line in Figure 4a). These features indicate that the CD signal splitting does not originate from the Cotton effect between stacked dye molecules, but from dyes in different environment.[69,70] Electrospray ionization mass spectrometry (ESI-MS) measurement suggests both ThT@β-CyD and ThT/SDS complexes come into formation with elevating temperature (Figure S8). In line with the formation of the two different complexes, considerable blue shift of the UV absorbance of ThT was observed[71,72] (Figure S9). Meanwhile, fluorescence measurements (lower panel of Figure 4b) revealed that the emission blue-shifts from 574 to 494 nm with increasing temperature from 25 to 40 °C. Control experiments suggest that the emission of ThT@β-CyD and ThT/SDS complexes should occur at 494 and 503 nm, respectively, and both emissions do not blue shift with increasing temperature (Figure S10). This result supports strongly that the CD signal splitting is due to the formation of ThT/SDS complex and ThT@β-CyD complex.

This conclusion is further confirmed by the CPL measurements. The lower panel of Figure 4b shows that at temperature around 30 °C, the ThT@β-CyD complex on the tube wall
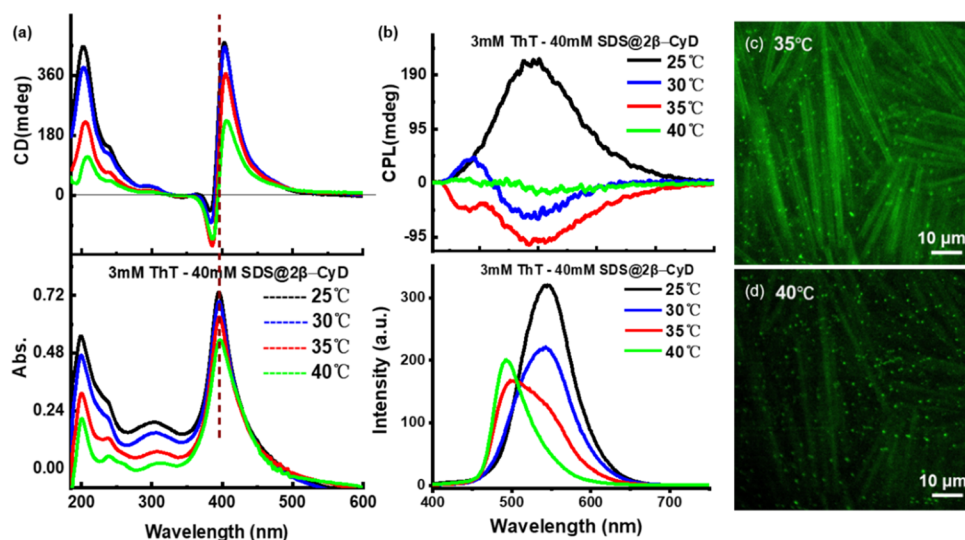
Figure 4. (a) CD and UV−vis spectra, (b) CPL spectra and FL emission, and (c, d) CLSM images of the microtubes composed of 3 mM ThT and 40 mM SDS@2β-CyD at different temperatures.
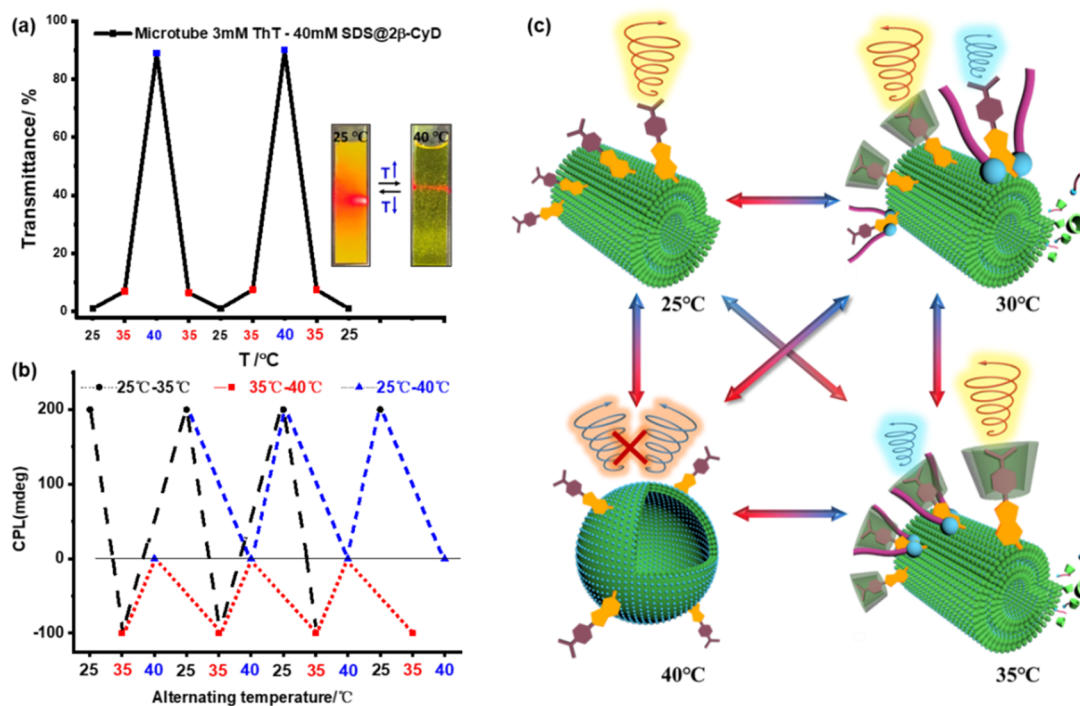

Figure 5. (a) Variation of the transmittance of the ThT-SDS@2β-CyD at 650 nm with varying temperature; (b) switchable CPL inversion cycles (at 590 nm) of 3 mM ThT/40 mM SDS@2β-CyD suspension by alternately changing temperature. The inset in (a) is the variation of the Tyndall effect of the sample. (c) Six basic CPL switching modes in different temperature combinations.

generates *r*-CPL at 570 nm, whereas the ThT/SDS complex gives *l*-CPL peaked at 494 nm[73] (Upper panel of Figure 4b, blue curve, and scheme in Figure 5c). It is striking that with further increasing temperature to around 35 °C, the *l*-CPL at 494 nm reverses to *r*-CPL, too. This CPL inversion means that the ThT molecules interacting with SDS has threaded into the cavity of β-CyD (scheme in Figure 5c), which is further evidenced by the ^{1}H NMR measurements in Figure S11. As a result, complete CPL handedness inversion occurs (upper panel of Figure 4b, red curve).

At temperatures above 40 °C, the CPL vanishes completely. TEM (Figure S12) and CLSM (Figures 4c, d and S13)

observation revealed that most of the tubes have transformed into vesicles around 200 nm (Figure S14, combination with DLS results). The vesicles start to from at 30 °C (Figures S12a and S13a), but tubes are still dominant in the temperature range of 30−35 °C. The population of vesicles becomes significant at temperatures above 40 °C (Figures S12d and Figure 4d). This means that the SDS@2β-CyD microtube structure is very crucial for the generation of CPL because it facilitates the ThT molecules to orient to the same direction. In contrast, when most of the tubes transform into vesicles around 200 nm at temperatures above 40 °C, the large curvature of a sphere force the ThT molecules orient to

different directions. As a result, CPL vanishes (Figure 4b, green line).

Because the temperature-triggered self-assembly transition is completely reversible (Figure 5a), the variation of the CPL strength and handedness is reversible too. Figure 5b shows the repeatable CPL emission at the wavelength of 494 and 570 nm at different temperature stages. The dissymmetric factor g_{em} is up to 0.11 for the l-CPL at 25 °C. Although the reversed r-CPL at 35 °C is separated into two groups peaked at 490 and 570 nm, respectively, the corresponding g_{em} values of −0.038 (490 nm) and −0.09 (570 nm) are still very significant, because the $|g_{em}|$ for most chiral organic emitters is on the order of $\sim 10^{-3}$ to $\sim 10^{-5}$.[37,74−76] This means that both the two CPL emissions can be used to store information, which is of special importance in creating advanced data encryption and data security materials.[33,77] Based on the data in Figure 4, 6 basic CPL switching modes are schemed in Figure 5c in the temperature range of 25−40 °C.

The strategy of CPL handedness switches in this work can be extended to other fluorescent dyes that could form host−guest complex with β-CyD. For instance, as ThT is replaced by another linear dye, acridine orange (AO), similar CPL inversion occurs (Figure S15). However, if the dye cannot form host−guest complex with β-CyD, such as Rhodamine B (RhB), no CPL inversion is observed (Figure S16).

CONCLUSIONS

In conclusion, the two scenarios of Harata−Kodaka's rule for the host−guest chemistry of cyclodextrins can be employed to create temperature responsive CPL materials. At room temperature, coassembling the fluorescent dye ThT on the crystalline self-assembly of SDS@2β-CyD microtubes allows the induced chirality of SDS to transfer to the dye so that the CPL handedness of ThT is determined by the induced chirality of SDS. At the higher temperature of 35 °C, part of the crystalline microtubes dissolve, and the host−guest interaction occurs between ThT and β-CyD. The CPL of ThT is then directly determined by its own induced chirality by β-CyD. Because the chromophore of SDS and ThT is inside and outside the cavity of β-CyD, respectively, CPL inversion occurs. Both scenarios in nature are caused by the dipole−dipole interaction between the electronic transition moment of the guest molecule ThT and the bonds composing the chiral host β-CyD. Upon selecting linear dye which is capable of forming host−guest inclusion complex with β-CyD, the crystalline self-assembly of SDS@2β-CyD microtubes are able to amplify the left-handed CPL at room temperature and the right-handed CPL at elevated temperature. We envision that the crystalline self-assembly based on the host−guest chemistry of CyDs would open up a paradigm leading to smart chiroptical, especially CPL, materials.

ASSOCIATED CONTENT

Supporting Information

The Supporting Information is available free of charge at https://pubs.acs.org/doi/10.1021/jacsau.0c00061.

> Illustrations, statistical analysis, molecular models, NMR titration results and spectra, ESI-MS results, UV−vis spectra, fluorescence emission spectra, TEM images, CLSM images, DLS test results, and CPL spectra (PDF)

AUTHOR INFORMATION

Corresponding Author

Yun Yan − *Beijing National Laboratory for Molecular Sciences (BNLMS), College of Chemistry and Molecular Engineering, Peking University, Beijing 100871, China;* ⊙ orcid.org/0000-0001-8759-3918; Email: yunyan@pku.edu.cn

Authors

Xuejiao Wang − *Beijing National Laboratory for Molecular Sciences (BNLMS), College of Chemistry and Molecular Engineering, Peking University, Beijing 100871, China*

Wanwan Zhi − *Beijing National Laboratory for Molecular Sciences (BNLMS), College of Chemistry and Molecular Engineering, Peking University, Beijing 100871, China*

Cheng Ma − *Beijing National Laboratory for Molecular Sciences (BNLMS), College of Chemistry and Molecular Engineering, Peking University, Beijing 100871, China*

Zhiyang Zhu − *Beijing National Laboratory for Molecular Sciences (BNLMS), College of Chemistry and Molecular Engineering, Peking University, Beijing 100871, China*

Weilin Qi − *Beijing National Laboratory for Molecular Sciences (BNLMS), College of Chemistry and Molecular Engineering, Peking University, Beijing 100871, China*

Jianbin Huang − *Beijing National Laboratory for Molecular Sciences (BNLMS), College of Chemistry and Molecular Engineering, Peking University, Beijing 100871, China*

Complete contact information is available at:
https://pubs.acs.org/10.1021/jacsau.0c00061

Author Contributions

X. Wang carried out most of the experiments and drafted this paper. W. Zhi. conducted the Tyndall effect measurements and CPL measurements. C. Ma composed all of the cartoons and conducted the fluorescence measurements. Z. Zhu repeated the fluorescent measurement. W. Qi conducted the control experiments on Xylene@α-CyD in the revision. J. Huang discussed the results. Y. Yan designed the work and wrote up the paper. All authors have given approval to the final version of the manuscript.

Notes

The authors declare no competing financial interest.

ACKNOWLEDGMENTS

REFERENCES

(1) Palmer, L. C.; Stupp, S. I. Molecular Self-Assembly into One-Dimensional Nanostructures. *Acc. Chem. Res.* **2008**, *41*, 1674−1684.

(2) Lee, C. C.; Grenier, C.; Meijer, E.; Schenning, A. P. Preparation and characterization of helical self-assembled nanofibers. *Chem. Soc. Rev.* **2009**, *38*, 671−683.

(3) Xu, Z.; Gao, C. Graphene chiral liquid crystals and macroscopic assembled fibres. *Nat. Commun.* **2011**, *2*, 571.

(4) Wang, Z.; Cheng, F.; Winsor, T.; Liu, Y. Optical chiral metamaterials: a review of the fundamentals, fabrication methods and applications. *Nanotechnology* **2016**, *27*, 412001.

(5) Seet, K. K.; Mizeikis, V.; Matsuo, S.; Juodkazis, S.; Misawa, H. Three-Dimensional Spiral-Architecture Photonic Crystals Obtained By Direct Laser Writing. *Adv. Mater.* **2005**, *17*, 541−545.

(6) Rekharsky, M. V.; Inoue, Y. Complexation thermodynamics of cyclodextrins. *Chem. Rev.* **1998**, *98*, 1875−1918.

(7) Connors, K. A. The stability of cyclodextrin complexes in solution. *Chem. Rev.* **1997**, *97*, 1325−1358.

(8) Kano, K. Mechanisms for chiral recognition by cyclodextrins. *J. Phys. Org. Chem.* **1997**, *10*, 286−291.

(9) Han, C.; Li, H. Chiral recognition of amino acids based on cyclodextrin-capped quantum dots. *Small* **2008**, *4*, 1344−1350.

(10) Xie, G.; Tian, W.; Wen, L.; Xiao, K.; Zhang, Z.; Liu, Q.; Hou, G.; Li, P.; Tian, Y.; Jiang, L. Chiral recognition of l-tryptophan with beta-cyclodextrin-modified biomimetic single nanochannel. *Chem. Commun.* **2015**, *51*, 3135−3138.

(11) Takahashi, K. Organic reactions mediated by cyclodextrins. *Chem. Rev.* **1998**, *98*, 2013−2034.

(12) Brimioulle, R.; Lenhart, D.; Maturi, M. M.; Bach, T. Enantioselective Catalysis of Photochemical Reactions. *Angew. Chem., Int. Ed.* **2015**, *54*, 3872−3890.

(13) Takahashi, K.; Hattori, K. Asymmetric reactions with cyclodextrins. *J. Inclusion Phenom. Mol. Recognit. Chem.* **1994**, *17*, 1−24.

(14) Rau, H. Asymmetric photochemistry in solution. *Chem. Rev.* **1983**, *83*, 535−547.

(15) Harata, K.; Uedaira, H. The Circular Dichroism Spectra of the β-Cyclodextrin Complex with Naphthalene Derivatives. *Bull. Chem. Soc. Jpn.* **1975**, *48*, 375−378.

(16) Harata, K. Induced circular dichroism of cycloamylose complexes with meta- and para-disubstituted benzenes. *Bioorg. Chem.* **1981**, *10*, 255−265.

(17) Kodaka, M. A general rule for circular dichroism induced by a chiral macrocycle. *J. Am. Chem. Soc.* **1993**, *115*, 3702−3705.

(18) Kodaka, M. Sign of circular dichroism induced by.beta.-cyclodextrin. *J. Phys. Chem.* **1991**, *95*, 2110−2112.

(19) Bakirci, H.; Zhang, X.; Nau, W. M. Induced Circular Dichroism and Structural Assignment of the Cyclodextrin Inclusion Complexes of Bicyclic Azoalkanes. *J. Org. Chem.* **2005**, *70*, 39−46.

(20) Mendicuti, F.; González-Álvarez, M. J. Supramolecular Chemistry: Induced Circular Dichroism to Study Host−Guest Geometry. *J. Chem. Educ.* **2010**, *87*, 965−968.

(21) Krishnan, R.; Rakhi, A. M.; Gopidas, K. R. Study of β-cyclodextrin−Pyromellitic diimide complexation. Conformational analysis of binary and ternary complex structures by induced circular dichroism and 2D NMR spectroscopies. *J. Phys. Chem. C* **2012**, *116*, 25004−25014.

(22) Park, J. W.; Lee, S. Y.; Song, H. J.; Park, K. K. Self-Inclusion Behavior and Circular Dichroism of Aliphatic Chain-Linked β-Cyclodextrin−Viologen Compounds and Their Reduced Forms Depending on the Side of Modification. *J. Org. Chem.* **2005**, *70*, 9505−9513.

(23) Zhang, X.; Nau, W. M. Chromophore alignment in a chiral host provides a sensitive test for the orientation−intensity rule of induced circular dichroism. *Angew. Chem., Int. Ed.* **2000**, *39*, 544−547.

(24) Sun, M.; Xu, L.; Qu, A.; Zhao, P.; Hao, T.; Ma, W.; Hao, C.; Wen, X.; Colombari, F. M.; de Moura, A. F. Site-selective photoinduced cleavage and profiling of DNA by chiral semiconductor nanoparticles. *Nat. Chem.* **2018**, *10*, 821.

(25) Zinna, F.; Di Bari, L. Lanthanide Circularly Polarized Luminescence: Bases and Applications. *Chirality* **2015**, *27*, 1−13.

(26) Geng, Y.; Trajkovska, A.; Culligan, S. W.; Ou, J. J.; Chen, H. M. P.; Katsis, D.; Chen, S. H. Origin of Strong Chiroptical Activities in Films of Nonafluorenes with a Varying Extent of Pendant Chirality. *J. Am. Chem. Soc.* **2003**, *125*, 14032−14038.

(27) Li, M.; Li, S.-H.; Zhang, D.; Cai, M.; Duan, L.; Fung, M.-K.; Chen, C.-F. Stable Enantiomers Displaying Thermally Activated Delayed Fluorescence: Efficient OLEDs with Circularly Polarized Electroluminescence. *Angew. Chem., Int. Ed.* **2018**, *57*, 2889−2893.

(28) Kim, D.-Y., Potential application of spintronic light-emitting diode to binocular vision for three-dimensional display technology. *J. Korean Phys. Soc.* **2006**, *49*.

(29) Schadt, M. Liquid crystal materials and liquid crystal displays. *Annu. Rev. Mater. Sci.* **1997**, *27*, 305−379.

(30) Zhang, Y. P.; Chodavarapu, V. P.; Kirk, A. G.; Andrews, M. P. Nanocrystalline cellulose for covert optical encryption. *Proc. SPIE* **2012**, *6* (1−10), 10.

(31) Li, J.; Kamin, S.; Zheng, G.; Neubrech, F.; Zhang, S.; Liu, N. Addressable metasurfaces for dynamic holography and optical information encryption. *Sci. Adv.* **2018**, *4*, eaar6768.

(32) Wang, C.; Fei, H.; Qiu, Y.; Yang, Y.; Wei, Z.; Tian, Y.; Chen, Y.; Zhao, Y. Photoinduced birefringence and reversible optical storage in liquid-crystalline azobenzene side-chain polymers. *Appl. Phys. Lett.* **1999**, *74*, 19−21.

(33) Wagenknecht, C.; Li, C.-M.; Reingruber, A.; Bao, X.-H.; Goebel, A.; Chen, Y.-A.; Zhang, Q.; Chen, K.; Pan, J.-W. Experimental demonstration of a heralded entanglement source. *Nat. Photonics* **2010**, *4*, 549−552.

(34) Li, F.; Li, Y.; Wei, G.; Wang, Y.; Li, S.; Cheng, Y. Circularly Polarized Luminescence of Chiral Perylene Diimide Based Enantiomers Triggered by Supramolecular Self-Assembly. *Chem. - Eur. J.* **2016**, *22*, 12910−12915.

(35) Sang, Y.; Han, J.; Zhao, T.; Duan, P.; Liu, M. Circularly Polarized Luminescence in Nanoassemblies: Generation, Amplification, and Application. *Adv. Mater.* **2020**, *32*, 1900110.

(36) Takaishi, K.; Iwachido, K.; Ema, T. Solvent-Induced Sign Inversion of Circularly Polarized Luminescence: Control of Excimer Chirality by Hydrogen Bonding. *J. Am. Chem. Soc.* **2020**, *142*, 1774−1779.

(37) Mizusawa, T.; Sato, T.; Kitayama, Y.; Tajima, N.; Fujiki, M.; Imai, Y. Solvent- and Substituent−controlled Circularly Polarised Luminescence of C2-symmetric Binaphthyl Fluorophores. *ChemistrySelect* **2016**, *1*, 3398−3404.

(38) Ye, Q.; Zheng, F.; Zhang, E.; Bisoyi, H. K.; Zheng, S.; Zhu, D.; Lu, Q.; Zhang, H.; Li, Q. Solvent polarity driven helicity inversion and circularly polarized luminescence in chiral aggregation induced emission fluorophores. *Chemical Science* **2020**, *11*, 9989−9993.

(39) Niu, D.; Jiang, Y.; Ji, L.; Ouyang, G.; Liu, M. Self-Assembly through Coordination and π-Stacking: Controlled Switching of Circularly Polarized Luminescence. *Angew. Chem., Int. Ed.* **2019**, *58*, 5946−5950.

(40) Niu, D.; Ji, L.; Ouyang, G.; Liu, M. Histidine Proton Shuttle-Initiated Switchable Inversion of Circularly Polarized Luminescence. *ACS Appl. Mater. Interfaces* **2020**, *12*, 18148−18156.

(41) Lin, W. B.; He, D. Q.; Lu, H. Y.; Hu, Z. Q.; Chen, C. F. Sign inversions of circularly polarized luminescence for helical compounds by chemically fine-tuning operations. *Chem. Commun.* **2020**, *56*, 1863−1866.

(42) Wang, Y.; Jiang, Y.; Zhu, X.; Liu, M. Significantly Boosted and Inversed Circularly Polarized Luminescence from Photogenerated Radical Anions in Dipeptide Naphthalenediimide Assemblies. *J. Phys. Chem. Lett.* **2019**, *10*, 5861−5867.

(43) Gong, J.; Yu, M.; Wang, C.; Tan, J.; Wang, S.; Zhao, S.; Zhao, Z.; Qin, A.; Tang, B.; Zhang, X. Reaction-based chiroptical sensing of ClO− using circularly polarized luminescence via self-assembly organogel. *Chem. Commun.* **2019**, *55*, 10768−10771.

(44) Wang, F.; Ji, W.; Yang, P.; Feng, C.-L. Inversion of Circularly Polarized Luminescence of Nanofibrous Hydrogels through Co-assembly with Achiral Coumarin Derivatives. *ACS Nano* **2019**, *13*, 7281−7290.

(45) Li, P.; Lü, B.; Han, D.; Duan, P.; Liu, M.; Yin, M. Stoichiometry-controlled inversion of circularly polarized luminescence in co-assembly of chiral gelators with an achiral tetraphenylethylene derivative. *Chem. Commun.* **2019**, *55*, 2194−2197.

(46) Yang, L.; Wang, F.; Auphedeous, D.-i. Y.; Feng, C. Achiral isomers controlled circularly polarized luminescence in supramolecular hydrogels. *Nanoscale* **2019**, *11*, 14210−14215.

(47) Song, F.; Cheng, Y.; Liu, Q.; Qiu, Z.; Lam, J. W. Y.; Lin, L.; Yang, F.; Tang, B. Z. Tunable circularly polarized luminescence from molecular assemblies of chiral AIEgens. *Mat Chem. Front* **2019**, *3*, 1768−1778.

(48) Jin, X.; Yang, D.; Jiang, Y.; Duan, P.; Liu, M. Light-triggered self-assembly of a cyanostilbene-conjugated glutamide from nanobelts to nanotoroids and inversion of circularly polarized luminescence. *Chem. Commun.* **2018**, *54*, 4513−4516.

(49) Qiao, J.; Lin, S.; Li, J.; Tian, J.; Guo, J. Reversible chirality inversion of circularly polarized luminescence in a photo-invertible helical cholesteric superstructure. *Chem. Commun.* **2019**, *55*, 14590−14593.

(50) Yuan, C.-l.; Huang, W.; Zheng, Z.-g.; Liu, B.; Bisoyi, H. K.; Li, Y.; Shen, D.; Lu, Y.; Li, Q. Stimulated transformation of soft helix among helicoidal, heliconical, and their inverse helices. *Sci. Adv.* **2019**, *5*, eaax9501.

(51) Bisoyi, H. K.; Bunning, T. J.; Li, Q. Stimuli-Driven Control of the Helical Axis of Self-Organized Soft Helical Superstructures. *Adv. Mater.* **2018**, *30*, 1706512.

(52) Bisoyi, H. K.; Li, Q. Light-Directed Dynamic Chirality Inversion in Functional Self-Organized Helical Superstructures. *Angew. Chem., Int. Ed.* **2016**, *55*, 2994−3010.

(53) Jiang, H.; Jiang, Y.; Han, J.; Zhang, L.; Liu, M. Helical Nanostructures: Chirality Transfer and a Photodriven Transformation from Superhelix to Nanokebab. *Angew. Chem. Int. Edit* **2019**, *131*, 795−800.

(54) Rybicka, A.; Longhi, G.; Castiglioni, E.; Abbate, S.; Dzwolak, W.; Babenko, V.; Pecul, M. Thioflavin T: Electronic Circular Dichroism and Circularly Polarized Luminescence Induced by Amyloid Fibrils. *ChemPhysChem* **2016**, *17*, 2931−2937.

(55) Jiang, L.; Peng, Y.; Yan, Y.; Deng, M.; Wang, Y.; Huang, J. Annular Ring" microtubes formed by SDS@ 2β-CD complexes in aqueous solution. *Soft Matter* **2010**, *6*, 1731−1736.

(56) Jiang, L.; Peng, Y.; Yan, Y.; Huang, J. Aqueous self-assembly of SDS@ 2 β-CD complexes: lamellae and vesicles. *Soft Matter* **2011**, *7*, 1726−1731.

(57) Zhou, C.; Cheng, X.; Yan, Y.; Wang, J.; Huang, J. Reversible Transition between SDS@2β-CD Microtubes and Vesicles Triggered by Temperature. *Langmuir* **2014**, *30*, 3381−3386.

(58) Liang, J.; Guo, P.; Qin, X.; Gao, X.; Ma, K.; Zhu, X.; Jin, X.; Xu, W.; Jiang, L.; Duan, P. Hierarchically Chiral Lattice Self-Assembly Induced Circularly Polarized Luminescence. *ACS Nano* **2020**, *14*, 3190−3198.

(59) Yan, Y.; Hoffmann, H.; Makarsky, A.; Richter, W.; Talmon, Y. Swelling of Lα-Phases by Matching the Refractive Index of the Water−Glycerol Mixed Solvent and that of the Bilayers in the Block Copolymer System of (EO)15−(PDMS)15−(EO)15. *J. Phys. Chem. B* **2007**, *111*, 6374−6382.

(60) Helfrich, W. Steric Interaction of Fluid Membranes in Multilayer Systems. *Z. Naturforsch., A: Phys. Sci.* **1978**, *33*, 305.

(61) Longhi, G.; Castiglioni, E.; Koshoubu, J.; Mazzeo, G.; Abbate, S. Circularly Polarized Luminescence: A Review of Experimental and Theoretical Aspects. *Chirality* **2016**, *28*, 696−707.

(62) Richardson, F. S.; Riehl, J. P. Circularly polarized luminescence spectroscopy. *Chem. Rev.* **1977**, *77*, 773−792.

(63) Riehl, J. P.; Richardson, F. S. Circularly polarized luminescence spectroscopy. *Chem. Rev.* **1986**, *86*, 1−16.

(64) Singh, P. K.; Kumbhakar, M.; Pal, H.; Nath, S. Confined ultrafast torsional dynamics of Thioflavin-T in a nanocavity. *Phys. Chem. Chem. Phys.* **2011**, *13*, 8008−8014.

(65) Pescitelli, G.; Di Bari, L.; Berova, N. Application of electronic circular dichroism in the study of supramolecular systems. *Chem. Soc. Rev.* **2014**, *43*, 5211−5233.

(66) Jiang, L.; Peng, Y.; Yan, Y.; Huang, J. Aqueous self-assembly of SDS@2β-CD complexes: lamellae and vesicles. *Soft Matter* **2011**, *7*, 1726−1731.

(67) Jiang, L.; Yan, Y.; Huang, J. Versatility of cyclodextrins in self-assembly systems of amphiphiles. *Adv. Colloid Interface Sci.* **2011**, *169*, 13−25.

(68) Zhou, C.; Cheng, X.; Yan, Y.; Wang, J.; Huang, J. Reversible transition between SDS@ 2β-CD microtubes and vesicles triggered by temperature. *Langmuir* **2014**, *30*, 3381−3386.

(69) Shi, Y.-M.; Hu, K.; Pescitelli, G.; Liu, M.; Li, X.-N.; Du, X.; Xiao, W.-L.; Sun, H.-D.; Puno, P.-T. Schinortriterpenoids with Identical Configuration but Distinct ECD Spectra Generated by Nondegenerate Exciton Coupling. *Org. Lett.* **2018**, *20*, 1500−1504.

(70) Berova, N.; Harada, N.; Nakanishi, K. Exciton Coupling. In *Encyclopedia of Spectroscopy and Spectrometry*, 3rd ed.; Lindon, J. C., Tranter, G. E., Koppenaal, D. W., Eds.; Academic Press: Oxford, 2017; pp 539−557.

(71) Kumar, S.; Singh, A. K.; Krishnamoorthy, G.; Swaminathan, R. Thioflavin T Displays Enhanced Fluorescence Selectively Inside Anionic Micelles and Mammalian Cells. *J. Fluoresc.* **2008**, *18*, 1199−1205.

(72) Cundall, R. B.; Davies, A. K.; Morris, P. G.; Williams, J. Factors influencing the photosensitizing properties and photoluminescence of thioflavin T. *J. Photochem.* **1981**, *17*, 369−376.

(73) Singh, P. K.; Nath, S. Molecular Recognition Controlled Delivery of a Small Molecule from a Nanocarrier to Natural DNA. *J. Phys. Chem. B* **2013**, *117*, 10370−10375.

(74) Nakamura, M.; Suzuki, J.; Ota, F.; Takada, T.; Akagi, K.; Yamana, K. Helically assembled pyrene arrays on an RNA duplex that exhibit circularly polarized luminescence with excimer formation. *Chem. - Eur. J.* **2016**, *22*, 9121−9124.

(75) Kumar, J.; Nakashima, T.; Kawai, T. Circularly Polarized Luminescence in Chiral Molecules and Supramolecular Assemblies. *J. Phys. Chem. Lett.* **2015**, *6*, 3445−3452.

(76) Kimoto, T.; Amako, T.; Tajima, N.; Kuroda, R.; Fujiki, M.; Imai, Y. Control of Solid-state Circularly Polarized Luminescence of Binaphthyl Organic Fluorophores through Environmental Changes. *Asian J. Org. Chem.* **2013**, *2*, 404−410.

(77) Zheng, H.; Li, W.; Li, W.; Wang, X.; Tang, Z.; Zhang, S. X.-A.; Xu, Y. Uncovering the Circular Polarization Potential of Chiral Photonic Cellulose Films for Photonic Applications. *Adv. Mater.* **2018**, *30*, 1705948.